

EVA-CLIP: Improved Training Techniques for CLIP at Scale

Quan Sun¹ Yuxin Fang^{1,2} Ledell Wu¹ Xinlong Wang¹ Yue Cao¹

¹Beijing Academy of Artificial Intelligence ²Huazhong University of Science and Technology

Fight together with Rei at [baaivision/EVA/CLIP](https://github.com/baaivision/EVA/CLIP)

Abstract

Contrastive language-image pre-training, CLIP for short, has gained increasing attention for its potential in various scenarios. In this paper, we propose **EVA-CLIP**, a series of models that significantly improve the efficiency and effectiveness of CLIP training. Our approach incorporates new techniques for representation learning, optimization, and augmentation, enabling **EVA-CLIP** to achieve superior performance compared to previous CLIP models with the same number of parameters but significantly smaller training costs. Notably, our largest 5.0B-parameter **EVA-02-CLIP-E/14+** with only 9 billion seen samples achieves **82.0%** zero-shot top-1 accuracy on ImageNet-1K val. A smaller **EVA-02-CLIP-L/14+** with only 430 million parameters and 6 billion seen samples achieves **80.4%** zero-shot top-1 accuracy on ImageNet-1K val. To facilitate open access and open research, we release the complete suite of **EVA-CLIP** to the community.

1. Introduction

CLIP (Contrastive Language-Image Pre-training) is a powerful vision-language foundation model that leverages large-scale datasets to learn rich visual representations by bridging vision and language via contrastive image-text pre-training. The CLIP model exhibits robust zero-shot transferability [39], and has the potential to enhance both multimodal and unimodal visual tasks, such as AI-generated content applications [41, 20, 32, 45]. Despite its significance, training CLIP models remains an inevitable challenge due to its high computational cost and training instability issues when scaling up.

In this paper, we propose **EVA-CLIP**, a family of models that provides a feasible, efficient, and effective solution for training CLIP models. Our approach incorporates several techniques that can significantly reduce training costs, stabilize the training process and improve zero-shot performance, including initialize CLIP with pre-trained EVA [20, 19] representations, the LAMB [52] optimizer, randomly dropping

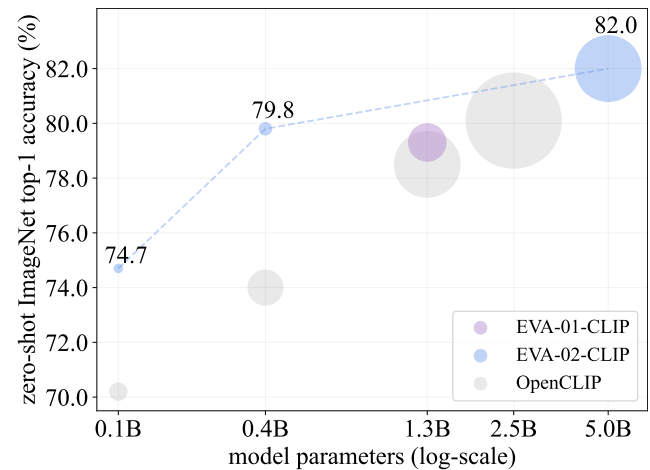


Figure 1: **Summary of CLIP models' ImageNet-1K zero-shot classification performance.** The diameter of each circle corresponds to forward GFLOPs x the number of training samples.

input tokens [33], and a speedup trick named flash attention [15]. With these techniques, we are able to greatly stabilize the training of CLIP models at scale with less computational costs and outperform the training-from-scratch counterpart with much fewer samples on a broad range of zero-shot benchmarks. Our largest 5.0B-parameter **EVA-02-CLIP-E/14+** with only 9 billion seen samples achieves 82.0% zero-shot top-1 accuracy on ImageNet-1K val. A smaller **EVA-02-CLIP-L/14+** with only 430 million parameters and 6 billion seen samples achieves 80.4% zero-shot top-1 accuracy on ImageNet-1K val.

2. Approach

Training CLIP [39] models is very hard and costly. The need for a large batch size and scaling up CLIP models can lead to significant computational resource requirements and even instability training problem. Fortunately, **EVA-CLIP** offers a highly efficient and effective solution that

model	precision	total #param.	image #param.	text #param.	data	samples seen	image size	batch size	gpus for training	IN-1K zs top-1
(a) comparisons with CLIP-Base baselines										
OpenAI CLIP-B/16	float16	149M	86M	63M	CLIP-400M	13B	224 ²	32k	unknown	68.3
EVA-01-CLIP-B/16	float16	149M	86M	63M	Merged-2B	3B	224 ²	32k	16×A100 (40GB)	69.7
Open CLIP-B/16	float16	149M	86M	63M	LAION-2B	34B	224 ²	88k	344×A100 (40GB)	70.2
EVA-02-CLIP-B/16	float16	149M	86M	63M	Merged-2B	8B	224 ²	131k	64×A100 (40GB)	74.7
(b) comparisons with CLIP-Large baselines										
Open CLIP-L/14	float16	428M	304M	124M	LAION-2B	32B	224 ²	79k	384×A100 (40GB)	74.0
OpenAI CLIP-L/14	float16	428M	304M	124M	CLIP-400M	13B	224 ²	32k	256×V100 (32GB)	75.5
EVA-02-CLIP-L/14	float16	428M	304M	124M	Merged-2B	4B	224 ²	131k	128×A100 (40GB)	79.8
(c) comparisons with larger CLIPs trained with more samples										
OpenAI CLIP-L/14+	float16	428M	304M	124M	CLIP-400M	13B	336 ²	32k	256×V100 (32GB)	76.6
Open CLIP-H/14	bfloat16	1.0B	632M	354M	LAION-2B	32B	224 ²	79k	824×A100 (40GB)	78.0
Open CLIP-g/14	bfloat16	1.3B	1.0B	354M	LAION-2B	34B	224 ²	88k	unknown	78.5
EVA-01-CLIP-g/14	float16	1.1B	1.0B	124M	LAION-400M	11B	224 ²	41k	256×A100 (40GB)	78.5
EVA-01-CLIP-g/14+	float16	1.3B	1.0B	354M	Merged-2B	11B	224 ²	114k	112×A100 (40GB)	79.3
Open CLIP-G/14	bfloat16	2.5B	1.8B	695M	LAION-2B	39B	224 ²	160k	512×A100 (80GB)	80.1
EVA-02-CLIP-L/14+	float16	428M	304M	124M	Merged-2B	6B	336 ²	61k	128×A100 (40GB)	80.4
EVA-02-CLIP-E/14	float16	4.7B	4.4B	354M	LAION-2B	4B	224 ²	115k	144×A100 (80GB)	81.9
EVA-02-CLIP-E/14+	bfloat16	5.0B	4.4B	695M	LAION-2B	9B	224 ²	144k	144×A100 (80GB)	82.0

(a) **CLIP model configurations and zero-shot top-1 accuracy on ImageNet.** With all techniques, **EVA-01-CLIP-g/14** can be stably trained via pure fp16 precision with fewer image-text pairs (11B v.s. 32B) sampled on $\sim 1/7 \times$ GPUs compared with Open CLIP-H/14. **EVA-01-CLIP-g/14** with smaller text encoder (124M v.s. 354M) was trained on a smaller dataset (LAION-400M v.s. LAION-2B) and only used the DeepSpeed optimization library [43] with ZeRO stage-1 optimizer [40]. **EVA-02-CLIP-E/14** with smaller text encoder (354M v.s. 695M) was trained with pure fp16.

method	IN-1K	IN-A	IN-R	IN-V2	IN-Sketch	ObjectNet	$\Delta\downarrow$	avg. acc.
(a) comparisons with CLIP-Base baselines								
OpenAI CLIP-B/16	68.3	50.0	77.7	61.9	48.2	55.3	8.1	60.2
Open CLIP-B/16	70.2	38.2	80.6	62.3	56.1	56.0	9.6	60.6
EVA-02-CLIP-B/16	74.7	54.1	82.5	67.0	57.7	62.3	8.3	66.4
(b) comparisons with CLIP-Large baselines								
Open CLIP-L/14	74.0	48.0	86.5	66.4	61.8	61.1	7.7	66.3
OpenAI CLIP-L/14	75.5	70.8	87.8	69.9	59.6	69.0	3.4	72.1
EVA-02-CLIP-L/14	79.8	76.1	92.7	72.9	68.1	75.3	2.9	77.5
(c) comparisons with larger CLIPs trained with more samples								
Open CLIP-H/14	78.0	59.3	89.3	70.9	66.6	69.7	5.7	72.3
Open CLIP-g/14	78.5	60.8	90.2	71.7	67.5	69.2	5.5	73.0
OpenAI CLIP-L/14+	76.6	77.5	89.0	70.9	61.0	72.0	2.1	74.5
EVA-01-CLIP-g/14	78.5	73.6	92.5	71.5	67.3	72.3	2.5	76.0
Open CLIP-G/14	80.1	69.3	92.1	73.6	68.9	73.0	3.9	76.2
EVA-01-CLIP-g/14+	79.3	74.1	92.5	72.1	68.1	75.3	2.4	76.9
EVA-02-CLIP-L/14+	80.4	82.9	93.2	73.8	68.9	78.4	0.8	79.6
EVA-02-CLIP-E/14	81.9	80.4	94.1	75.4	71.8	76.9	1.8	80.1
EVA-02-CLIP-E/14+	82.0	82.1	94.5	75.7	71.6	79.6	1.1	80.9

(b) **Summary of zero-shot performance on ImageNet variants and ObjectNet.** “avg. acc.”: the averaged top-1 accuracy on different ImageNet variants (*i.e.*, IN-{1K, V2, ReaL, Adv., Ren., Ske.}), and ObjectNet. “ $\Delta\downarrow$ ”: The gap between the averaged top-1 accuracy and the ImageNet-1K top-1 accuracy (the lower the better). **EVA-CLIP** suffers from the smallest performance drop (only **0.8%** top-1 accuracy gap for **EVA-02-CLIP-L/14+** and **1.1%** for **EVA-02-CLIP-E/14+**) while **EVA-02-CLIP-E/14+** achieves the highest zero-shot classification accuracy averaged on all 6 benchmarks (**80.9%** averaged top-1 accuracy).

Table 1: **CLIP model configurations and highlights of our key results.** Shown are the top-1 accuracy of our method, **EVA-CLIP**, and similar baselines – CLIP and Open CLIP – on ImageNet and other robustness test sets. None of these models have learned from any labeled training example in ImageNet.

significantly reduces the computational cost while achieving superior zero-shot performance across a broad range of benchmarks.

Better Initialization. To improve feature representation and expedite convergence of CLIP models, we adopt pre-trained EVA [20, 19] models which combines high-level

	ImageNet-1K [16]	ImageNet-V2 [44]	ImageNet-Adv. [25]	ImageNet-Ren. [24]	ImageNet-Ske. [50]	ObjectNet [3]	CIFAR-10 [30]	CIFAR-100 [30]	MINIST [31]	Caltech-101 [21]	SUN397 [51]	FGVC Aircraft [36]	Country-211 [39]	Stanford Cars [29]	Birdsnap [4]	DTD [12]	Eurosat [23]	FER2013 [22]	Flowers-102 [37]	Food-101 [5]	GTSRB [48]	PCam [49]	Pets [38]	Rendered SST2 [39]	Resisc45 [11]	STL10 [14]	VOC2017 [18]	avg. top-1 acc.
(a) comparisons with CLIP-Base baselines																												
OpenAI CLIP-B/16	68.3	61.9	50.0	77.7	48.2	55.3	90.8	67.0	51.6	84.7	64.4	24.4	22.8	64.8	34.5	44.7	55.0	46.2	71.3	88.8	43.5	50.7	89.1	60.8	59.1	98.3	78.3	61.2
Open CLIP-B/16	70.2	62.3	38.2	80.6	56.1	56.0	94.9	76.9	65.9	86.7	70.8	27.0	20.3	88.5	42.1	56.6	52.7	51.8	71.4	86.6	48.3	56.3	90.3	60.0	63.4	97.9	70.8	64.5
EVA-02-CLIP-B/16	74.7	67.0	54.1	82.5	57.7	62.3	98.4	87.7	47.9	86.3	70.7	24.8	21.4	78.6	37.7	53.1	67.0	51.2	75.9	89.4	46.3	50.9	92.2	54.1	60.7	99.5	80.2	65.6
(b) comparisons with CLIP-Large baselines																												
OpenAI CLIP-L/14	75.5	69.9	70.8	87.8	59.6	69.0	95.6	75.8	76.4	86.7	67.6	31.4	31.9	77.9	40.5	55.4	62.4	49.9	79.2	93.1	50.6	52.0	93.5	68.9	64.6	99.4	67.6	69.0
Open CLIP-L/14	74.0	66.4	48.0	86.5	61.8	61.1	95.8	78.4	64.4	87.6	74.0	34.8	24.4	91.5	45.2	61.5	57.8	50.9	74.4	88.8	51.6	55.5	92.8	60.3	67.3	98.5	74.0	67.9
EVA-02-CLIP-L/14	79.8	72.9	76.1	92.7	68.1	75.3	99.1	90.7	67.3	88.3	74.1	36.2	30.9	90.5	43.8	63.2	70.0	53.4	77.0	93.4	57.1	54.2	93.9	61.6	70.0	99.6	82.2	72.6
(c) comparisons with larger CLIPs trained with more samples																												
OpenAI CLIP-L/14+	76.6	70.9	77.5	89.0	61.0	72.0	94.9	74.4	79.0	87.2	68.7	33.4	34.5	79.3	41.0	56.0	61.5	49.1	78.6	93.9	52.4	60.8	93.8	70.7	65.4	99.4	78.1	70.3
EVA-01-CLIP-g/14	78.5	71.5	73.6	92.5	67.3	72.3	98.3	88.7	62.3	87.7	74.2	32.4	28.6	91.7	50.0	61.3	73.6	52.2	74.5	93.5	49.1	49.9	94.2	58.4	70.3	98.9	83.2	71.4
Open CLIP-g/14	78.5	71.7	60.8	90.2	67.5	69.2	98.2	84.7	71.9	88.1	74.1	44.6	30.9	94.0	51.0	68.7	64.7	55.8	81.0	92.4	49.7	53.8	93.9	56.7	69.6	98.9	81.6	71.9
Open CLIP-H/14	78.0	70.8	59.2	89.3	66.6	69.7	97.4	84.7	72.9	85.0	75.2	42.8	30.0	93.5	52.9	67.8	72.7	52.0	80.1	92.7	58.4	54.2	94.5	64.3	70.5	98.5	77.7	72.3
EVA-02-CLIP-L/14+	80.4	73.8	82.9	93.2	68.9	78.4	98.9	89.8	64.3	89.5	74.8	37.5	33.6	91.6	45.8	64.5	71.4	51.0	77.2	94.2	57.6	54.9	94.2	64.6	69.8	99.7	82.7	73.5
EVA-01-CLIP-g/14+	79.3	72.1	74.1	92.5	68.1	75.3	99.1	90.1	71.8	88.1	74.3	39.4	30.8	90.7	52.6	67.3	73.2	56.0	79.7	93.7	66.5	62.3	94.8	58.6	71.4	99.5	82.9	74.2
Open CLIP-G/14	80.1	73.6	69.3	92.1	68.9	73.0	98.2	87.5	71.6	86.4	74.5	49.7	33.8	94.5	54.5	69.0	70.0	59.5	81.5	93.1	62.5	63.6	95.2	65.2	72.6	98.5	80.7	74.8
EVA-02-CLIP-E/14	81.9	75.4	80.4	94.1	71.8	76.9	99.3	92.5	76.7	89.0	76.5	47.9	34.7	94.4	56.3	68.2	77.6	55.1	82.5	95.2	67.1	49.6	95.6	61.1	73.5	99.2	83.0	76.1
EVA-02-CLIP-E/14+	82.0	75.7	82.1	94.5	71.6	79.6	99.3	93.1	74.7	90.5	75.1	54.1	35.7	94.6	58.1	68.2	75.8	58.6	84.5	94.9	67.7	63.7	95.8	61.4	75.6	99.2	85.6	77.5

Table 2: Summary of EVA-CLIP zero-shot image classification performance on 27 datasets.

method	UCF-101	K-400	K-600	K-700	avg. acc.
(a) comparisons with CLIP-Base baselines					
Open CLIP-B/16	67.5	54.5	54.2	46.8	55.8
OpenAI CLIP-B/16	67.1	57.6	56.5	49.3	57.6
EVA-02-CLIP-B/16	68.6	57.4	57.0	50.0	58.3
(b) comparisons with CLIP-Large baselines					
Open CLIP-L/14	73.2	58.0	58.6	50.8	60.2
OpenAI CLIP-L/14	76.4	64.5	64.2	57.7	65.7
EVA-02-CLIP-L/14	76.8	65.0	64.9	59.1	66.5
(c) comparisons with larger CLIPs trained with more samples					
Open CLIP-H/14	78.2	63.1	63.6	56.1	65.3
Open CLIP-g/14	77.8	63.9	64.1	56.9	65.7
EVA-01-CLIP-g/14	76.0	65.2	64.4	58.4	66.0
OpenAI CLIP-L/14+	78.1	64.9	65.0	58.5	66.6
EVA-02-CLIP-L/14+	78.6	65.9	66.1	60.2	67.7
Open CLIP-G/14	80.5	65.9	66.1	59.2	67.9
EVA-01-CLIP-g/14+	78.9	66.7	67.0	60.9	68.4
EVA-02-CLIP-E/14	82.8	68.6	68.6	62.5	70.6
EVA-02-CLIP-E/14+	83.1	69.8	69.3	63.4	71.4

Table 3: Summary of EVA-CLIP zero-shot video classification performance.

semantics of image-text contrastive learning with geometric and structural capture from masked image modeling. We use pre-trained EVA weights to initialize the image encoder of EVA-CLIP. Our empirical study demonstrates that pre-trained EVA models not only help EVA-CLIP achieve superior performance on various zero-shot benchmarks but also

expedites and stabilizes the training process.

Optimizer. We use the LAMB [52] optimizer for training our EVA-CLIP models. LAMB optimizer is specifically designed for large-batch training, and its adaptive element-wise updating and layer-wise learning rates enhance training efficiency and accelerate convergence rates. Given the exceptionally large batch sizes used for training CLIP models, the original CLIP model uses a batch size of 32,768 and some open-sourced CLIP models even use an extremely large batch size of more than 100k. EVA-CLIP shows that LAMB optimizer is the preferred optimizer for training large-scale CLIP models.

FLIP [33] has shown promising results in large-scale settings. In this work, we leverage FLIP to improve the time efficiency of training CLIP models. Specifically, we randomly mask 50% image tokens during training resulting in a significant reduction of time complexity by half. This approach also allows for a $2\times$ increase in batch size, without any additional memory costs.

3. Experiments

Settings. In our experiments, we initialized the vision encoder with pre-trained weights from EVA [20, 19] and the text encoder with pre-trained weights from either OpenAI CLIP [39] or OpenCLIP [27]. Specifically, the vision encoder of EVA-01-CLIP is initialized from EVA-01 [20], and the vision encoder of EVA-02-CLIP is initialized from

method	zero-shot text retrieval						zero-shot image retrieval					
	Flickr30K			COCO			Flickr30K			COCO		
	R@1	R@5	R@10	R@1	R@5	R@10	R@1	R@5	R@10	R@1	R@5	R@10
(a) comparisons with CLIP- Base baselines												
OpenAI CLIP-B/16	81.9	96.2	98.8	52.4	76.8	84.7	62.1	85.6	91.8	33.1	58.4	69.0
Open CLIP-B/16	86.3	97.9	99.4	59.4	81.8	88.6	69.8	90.4	94.6	42.3	66.7	77.1
EVA-02-CLIP-B/16	85.7	96.7	98.9	58.7	80.7	88.2	71.2	91.0	94.7	42.2	66.9	76.3
(b) comparisons with CLIP- Large baselines												
OpenAI CLIP-L/14	85.2	97.3	99.0	56.3	79.3	86.7	65.2	87.3	92.0	36.5	61.0	71.1
Open CLIP-L/14	88.7	98.4	99.2	62.1	83.4	90.3	75.0	92.5	95.6	46.1	70.7	79.4
EVA-02-CLIP-L/14	89.7	98.6	99.2	63.7	84.3	90.4	77.3	93.6	96.8	47.5	71.2	79.7
(c) comparisons with larger CLIPs trained with more samples												
OpenAI CLIP-L/14+	87.4	98.3	99.3	57.9	81.2	87.9	67.3	89.0	93.3	37.1	61.6	71.5
Open CLIP-H/14	90.8	99.3	99.7	66.0	86.1	91.9	77.8	94.1	96.6	49.5	73.4	81.5
Open CLIP-g/14	91.4	99.2	99.6	66.4	86.0	91.8	77.7	94.1	96.9	48.8	73.3	81.5
Open CLIP-G/14	92.9	99.3	99.8	67.3	86.9	92.6	79.5	95.0	97.1	51.4	74.9	83.0
EVA-01-CLIP-g/14	88.3	98.3	99.3	61.8	83.3	90.0	72.6	91.6	95.1	44.1	68.5	77.3
EVA-01-CLIP-g/14+	91.6	99.3	99.8	68.2	87.5	92.5	78.9	94.5	96.9	50.3	74.0	82.1
EVA-02-CLIP-L/14+	89.2	98.9	99.6	64.1	85.2	90.8	77.9	94.2	96.8	47.9	71.7	80.0
EVA-02-CLIP-E/14	92.4	99.3	99.9	68.1	87.7	92.8	78.8	94.6	97.0	50.8	74.7	82.5
EVA-02-CLIP-E/14+	93.9	99.4	99.8	68.8	87.8	92.8	78.8	94.2	96.8	51.1	75.0	82.7

Table 4: Summary of zero-shot retrieval performance on Flickr30K [53] and COCO [34]

EVA-02 [19]. We adopt the LAMB optimizer with $\beta_1 = 0.9$, $\beta_2=0.98$, and a weight decay of 0.05. We applied different learning rates and layer decay rates to the vision encoder and text encoder to ensure optimal training. For example, we set the learning rate to $2e-4$ for the vision encoder and $2e-5$ for the text encoder of **EVA-01-CLIP-g** during the first 2000 warming-up steps. Afterward, we decayed the learning rate linearly to 0 for the remainder of the training steps. To further improve the training process, we used the DeepSpeed optimization library [43] with ZeRO stage-1 optimizer [40], gradient checkpointing [10] and flash attention [15] to save memory and accelerate training process. We found that using the fp16 precision with dynamic loss scaling was sufficiently stable throughout the **EVA-01-CLIP-g** training process, while bfloat16 format was necessary to stabilize the training process of **EVA-02-CLIP-E+**.

To construct our training dataset, Merged-2B, we merged 1.6 billion samples from LAION-2B [45] dataset with 0.4 billion samples from COYO-700M [6].

System-level Comparison. We present CLIP model configurations and zero-shot accuracies on ImageNet variants and ObjectNet in Table 1. **EVA-02-CLIP-E/14+** achieves the highest zero-shot top-1 accuracy of 80.9% averaged across all 6 benchmarks, with the smallest performance drop (1.1% top-1 accuracy gap). Notably, this result surpasses the previous largest and best open-sourced OpenCLIP-G/14 [1] by 1.9% on ImageNet and 4.7% on the average accuracy of 6 benchmarks. Remarkably, with those powerful techniques, the large size **EVA-02-CLIP-L** can even reach up to 80.4% zero-shot top-1 on ImageNet, outperforming OpenCLIP-G/14 with only $\sim 1/6$ parameters and $\sim 1/6$ image-text training

samples.

In Table 2, we further demonstrate the efficacy and robustness of our approach on all 27 zero-shot image classification benchmarks. Our largest **EVA-02-CLIP-E/14+** achieves averaged 77.5% on all 27 benchmarks. Notably, our **EVA-02-CLIP-L/14+** model, which only has $\sim 1/2$ of the model size and $\sim 1/5$ image-text pairs, achieves a 1.2-point averaged improvement over OpenCLIP-H/14.

For video classification, we sample only a single center frame in each video, making it an image classification task. Following the conventional settings, we report the top-1 accuracy for UCF-101 [47] and the mean of top-1 and top-5 accuracy for Kinetics-400 [9], Kinetics-600 [7] and Kinetics-700 [8]. In Table 3 we show that **EVA-CLIP** is also quite effective in zero-shot video recognition benchmarks.

Table 4 reports the zero-shot image and text retrieval results on Flickr30K [53] and COCO [34]. **EVA-CLIP** outperforms all the competitors at the base and large model size. While the zero-shot retrieval performance of **EVA-02-CLIP-E/14** is slightly lower than OpenCLIP-G/14, the results are still competitive. We speculate that the main reason is that retrieval tasks depend more on the capacity of the text encoder and the number of training samples, and in comparison, the capacity of the text encoder in **EVA-02-CLIP-E/14** is smaller and the number of training samples is less than that of OpenCLIP-G/14. To this end, we have trained **EVA-02-CLIP-E/14+** with a larger capacity text encoder and more training samples. The results show that this improved model can substantially improve retrieval performance and outperform OpenCLIP-G/14 on zero-shot text retrieval tasks.

method	dataset	EVA		mask 50%	samples seen	IN-1K zs top-1
		init	optimizer			
EVA-CLIP-B	LAION-400M	✗	AdamW	✗	13B	67.1
	LAION-400M	✓	AdamW	✗	5B	68.9
	LAION-400M	✓	LAMB	✗	5B	69.6
	LAION-400M	✓	LAMB	✓	5B	68.9
	LAION-2B	✓	LAMB	✓	5B	69.6
	merged-2B	✓	LAMB	✓	2.5B	69.7

Table 5: **Ablation Studies.** Our LAION-2B dataset comprises only 1.6B samples.

method	mask	flash	time / 40m samples	memory / GPU
	50%	attention		
EVA-CLIP-B	✗	✗	132min	33GB
	✗	✓	76min	26GB
	✓	✗	64min	18GB
	✓	✓	55min	16GB

Table 6: **Training time and GPU memory.** Training on 16 NVIDIA 40G-A100 GPUs with the DeepSpeed [43] ZeRO stage-1 optimizer [40] and gradient checkpointing [10]. The batch size is 32k.

Ablation Study. We first ablate the EVA-CLIP design in Table 5. The image encoder is ViT-B/16[17] model and text encoder is CLIP-B-16. We conducted experiments with a batch size of 32k and evaluated zero-shot accuracy on the ImageNet-1K validation set. It is important to note that we used a shorter training schedule than the final models.

We trained our model on the LAION-400M[46] dataset using the AdamW[35] optimizer. Comparing to training from scratch, EVA initialization resulted in a 1.8% increase in zero-shot top-1 accuracy on ImageNet with only $\sim 1/2$ seen samples.

Furthermore, we experimented with using the LAMB optimizer instead of AdamW with EVA initialization on the LAION-400M dataset. This resulted in a 0.7% increase in zero-shot top-1 accuracy on ImageNet with the same seen samples. When 50% masking was applied, the accuracy decreased by 0.7% while enjoying a speedup of $2\times$. These results highlight the significance of LAMB optimizer in training high-performing models and the strategy of masking image tokens in faster training without marginally decreasing accuracy.

We also conducted experiments with the LAION-2B dataset using EVA initialization, LAMB optimizer, and 50% masking, which increased the accuracy by 0.7% compared to LAION-400M. Only half samples were required to achieve the same top-1 accuracy when using the merged-2B dataset. It demonstrates the importance of dataset sizes and the significant convergence speed through merging the two datasets.

Computation Costs. In Table 6, we present the memory and time cost of our implementation. As shown, masking 50% of image tokens can accelerate training time by $2\times$ and using flash attention can reduce additional 15% training

method	image encoder			text encoder			# params		
	layers	width	heads	layers	width	heads	image	text	total
EVA-02-CLIP-B/16	12	768	12	12	512	8	86M	63M	149M
EVA-02-CLIP-L/14	24	1024	16	12	768	12	304M	124M	428M
EVA-01-CLIP-g/14	40	1408	16	12	768	12	1.0B	124M	1.1B
EVA-01-CLIP-g/14+	40	1408	16	24	1024	16	1.0B	354M	1.3B
EVA-02-CLIP-E/14	64	1792	16	24	1024	16	4.4B	354M	4.7B
EVA-02-CLIP-E/14+	64	1792	16	32	1280	20	4.4B	695M	5.0B

Table 7: **Architecture configurations.**

time.

Using all these techniques, we can train EVA-CLIP with a lower budget than other counterpart CLIP models. For instance, EVA-CLIP-B/16 can be trained on a batch size of 32k and converges within 300 hours using on 16 NVIDIA 40GB-A100 GPUs. Similarly, the billion-scale EVA CLIP-g/14 can be trained on a batch size of 65k and requires less than 25 days to train 12B samples using 64 NVIDIA 40G-A100 GPUs. These results demonstrate the scalability and effectiveness of our method in achieving state-of-the-art results while maintaining an optimal balance between training time and GPU memory utilization.

config	EVA-02-CLIP-B / -L / -L+
image enc. weight init.	EVA-02-B / -L / EVA-02-CLIP-L
text enc. weight init.	OpenAI CLIP-B / -L / EVA-02-CLIP-L
image-text data	Merged-2B
image enc. peak learning rate	$2e-4 / 4e-4 / 4e-4$
image enc. layer-wise lr decay [13, 2]	$0.75 / 0.85 / 0.75$
text enc. peak learning rate	$2e-5 / 4e-5 / 4e-5$
text enc. layer-wise lr decay [13, 2]	$0.75 / 0.75 / 0.65$
learning rate schedule	cosine decay
optimizer	LAMB [52]
optimizer hyper-parameters	$\beta_1, \beta_2, \epsilon = 0.9, 0.98, 1e-6$
weight decay	0.05
input resolution	$224^2 / 224^2 / 336^2$
patch size	$16^2 / 14^2 / 14^2$
batch size	131k / 131k / 61k
samples seen	8B / 4B / 2B
drop path [26]	0.0
random resized crop	(0.9, 1)
numerical precision	DeepSpeed fp16 [43]
ZeRO optimizer [42]	stage 1

Table 8: **EVA-CLIP-B and EVA-CLIP-L training setting.**

References

- [1] Reaching 80 zero-shot accuracy with openclip: Vit-g/14 trained on laion-2b. <https://laion.ai/blog/giant-openclip/>. 4
- [2] Hangbo Bao, Li Dong, and Furu Wei. Beit: Bert pre-training of image transformers. *arXiv preprint arXiv:2106.08254*, 2021. 5, 6
- [3] Andrei Barbu, David Mayo, Julian Alverio, William Luo, Christopher Wang, Dan Gutfreund, Josh Tenenbaum, and Boris Katz. Objectnet: A large-scale bias-controlled dataset for pushing the limits of object recognition models. In *NeurIPS*, 2019. 3
- [4] Thomas Berg, Jiongxin Liu, Seung Woo Lee, Michelle L Alexander, David W Jacobs, and Peter N Belhumeur. Birdsnap: Large-

config	EVA-01-CLIP-g / EVA-02-CLIP-g+
image enc. weight init.	EVA-01-g
text enc. weight init.	Openai CLIP-L / Open CLIP-H
image-text data	LAION-400M [46] / Merged-2B
image enc. peak learning rate	4e-4
image enc. layer-wise lr decay [13, 2]	0.85
text enc. peak learning rate	4e-5
text enc. layer-wise lr decay [13, 2]	0.75
learning rate schedule	cosine decay
optimizer	AadamW [28, 35] / LAMB [52]
optimizer hyper-parameters	$\beta_1, \beta_2, \epsilon = 0.9, 0.98, 1e-6$
weight decay	0.05
input resolution	224 ²
patch size	14 ²
batch size	41k / 114k
samples seen	11B / 11B
drop path [26]	0.0
random resized crop	(0.9, 1)
numerical precision	DeepSpeed fp16 [43]
ZeRO optimizer [42]	stage 1

Table 9: **EVA-CLIP-g and EVA-CLIP-g+ training setting.**

config	EVA-01-CLIP-E / EVA-02-CLIP-E+
image enc. weight init.	EVA-02-E
text enc. weight init.	Open CLIP-H / Open CLIP-G
image-text data	LAION-2B [45]
image enc. peak learning rate	4e-4
image enc. layer-wise lr decay [13, 2]	0.9
text enc. peak learning rate	4e-5
text enc. layer-wise lr decay [13, 2]	0.75
learning rate schedule	cosine decay
optimizer	LAMB [52]
optimizer hyper-parameters	$\beta_1, \beta_2, \epsilon = 0.9, 0.98, 1e-6$
weight decay	0.05
input resolution	224 ²
patch size	14 ²
batch size	115k / 144k
samples seen	4B / 9B
drop path [26]	0.0
random resized crop	(0.9, 1)
numerical precision	DeepSpeed fp16 / DeepSpeed bf16 [43]
ZeRO optimizer [42]	stage 1

Table 10: **EVA-CLIP-E and EVA-CLIP-E+ training setting.**

- scale fine-grained visual categorization of birds. In *CVPR*, 2014. 3
- [5] Lukas Bossard, Matthieu Guillaumin, and Luc Van Gool. Food-101—mining discriminative components with random forests. In *ECCV*, 2014. 3
- [6] Minwoo Byeon, Beomhee Park, Haecheon Kim, Sungjun Lee, Woonhyuk Baek, and Saehoon Kim. Coyo-700m: Image-text pair dataset. <https://github.com/kakaobrain/coyo-dataset>, 2022. 4
- [7] Joao Carreira, Eric Noland, Andras Banki-Horvath, Chloe Hillier, and Andrew Zisserman. A short note about kinetics-600. *arXiv preprint arXiv:1808.01340*, 2018. 4
- [8] Joao Carreira, Eric Noland, Chloe Hillier, and Andrew Zisserman. A short note on the kinetics-700 human action dataset. *arXiv preprint arXiv:1907.06987*, 2019. 4
- [9] Joao Carreira and Andrew Zisserman. Quo vadis, action recognition? a new model and the kinetics dataset. In *CVPR*, 2017. 4
- [10] Tianqi Chen, Bing Xu, Chiyuan Zhang, and Carlos Guestrin. Training deep nets with sublinear memory cost, 2016. 4, 5
- [11] Gong Cheng, Junwei Han, and Xiaoqiang Lu. Remote sensing image scene classification: Benchmark and state of the art. *Proceedings of the IEEE*, 2017. 3
- [12] M. Cimpoi, S. Maji, I. Kokkinos, S. Mohamed, , and A. Vedaldi. Describing textures in the wild. In *CVPR*, 2014. 3
- [13] Kevin Clark, Minh-Thang Luong, Quoc V Le, and Christopher D Manning. ELECTRA: Pre-training text encoders as discriminators rather than generators. *arXiv preprint arXiv:2003.10555*, 2020. 5, 6
- [14] Adam Coates, Andrew Ng, and Honglak Lee. An analysis of single-layer networks in unsupervised feature learning. In *AISTAT*, 2011. 3
- [15] Tri Dao, Daniel Y. Fu, Stefano Ermon, Atri Rudra, and Christopher Ré. Flashattention: Fast and memory-efficient exact attention with io-awareness, 2022. 1, 4
- [16] Jia Deng, Wei Dong, Richard Socher, Li-Jia Li, Kai Li, and Li Fei-Fei. Imagenet: A large-scale hierarchical image database. In *CVPR*, 2009. 3
- [17] Alexey Dosovitskiy, Lucas Beyer, Alexander Kolesnikov, Dirk Weissenborn, Xiaohua Zhai, Thomas Unterthiner, Mostafa Dehghani, Matthias Minderer, Georg Heigold, Sylvain Gelly, Jakob Uszkoreit, and Neil Houlsby. An image is worth 16x16 words: Transformers for image recognition at scale, 2020. 5
- [18] Mark Everingham, SM Ali Eslami, Luc Van Gool, Christopher KI Williams, John Winn, and Andrew Zisserman. The pascal visual object classes challenge: A retrospective. *IJCV*, 2015. 3
- [19] Yuxin Fang, Quan Sun, Xinggang Wang, Tiejun Huang, Xinlong Wang, and Yue Cao. Eva-02: A visual representation for neon genesis. *arXiv preprint arXiv:2303.11331*, 2023. 1, 2, 3, 4
- [20] Yuxin Fang, Wen Wang, Binhui Xie, Quan Sun, Ledell Wu, Xinggang Wang, Tiejun Huang, Xinlong Wang, and Yue Cao. Eva: Exploring the limits of masked visual representation learning at scale. *arXiv preprint arXiv:2211.07636*, 2022. 1, 2, 3
- [21] Li Fei-Fei, Rob Fergus, and Pietro Perona. Learning generative visual models from few training examples: An incremental bayesian approach tested on 101 object categories. In *CVPRW*, 2004. 3
- [22] Ian J Goodfellow, Dumitru Erhan, Pierre Luc Carrier, Aaron Courville, Mehdi Mirza, Ben Hamner, Will Cukierski, Yichuan Tang, David Thaler, Dong-Hyun Lee, et al. Challenges in representation learning: A report on three machine learning contests. In *ICONIP*, 2013. 3
- [23] Patrick Helber, Benjamin Bischke, Andreas Dengel, and Damian Borth. Eurosat: A novel dataset and deep learning benchmark for land use and land cover classification. *IEEE J. Sel. Top. Appl. Earth Obs. Remote Sens.*, 2019. 3
- [24] Dan Hendrycks, Steven Basart, Norman Mu, Saurav Kadavath, Frank Wang, Evan Dorundo, Rahul Desai, Tyler Zhu, Samyak Parajuli, Mike Guo, et al. The many faces of robustness: A critical analysis of out-of-distribution generalization. In *CVPR*, 2021. 3
- [25] Dan Hendrycks, Kevin Zhao, Steven Basart, Jacob Steinhardt, and Dawn Song. Natural adversarial examples. In *CVPR*, 2021. 3
- [26] Gao Huang, Yu Sun, Zhuang Liu, Daniel Sedra, and Kilian Q Weinberger. Deep networks with stochastic depth. In *ECCV*, 2016. 5, 6
- [27] Gabriel Ilharco, Mitchell Wortsman, Ross Wightman, Cade Gordon, Nicholas Carlini, Rohan Taori, Achal Dave, Vaishaal Shankar, Hongseok Namkoong, John Miller, Hannaneh Hajishirzi, Ali Farhadi, and Ludwig Schmidt. Openclip. https://github.com/mlfoundations/open_clip, 2021. 3

- [28] Diederik P Kingma and Jimmy Ba. Adam: A method for stochastic optimization. *arXiv preprint arXiv:1412.6980*, 2014. 6
- [29] Jonathan Krause, Michael Stark, Jia Deng, and Li Fei-Fei. 3d object representations for fine-grained categorization. In *ICCVW*, 2013. 3
- [30] Alex Krizhevsky, Geoffrey Hinton, et al. Learning multiple layers of features from tiny images. 2009. 3
- [31] Yann LeCun, Léon Bottou, Yoshua Bengio, and Patrick Haffner. Gradient-based learning applied to document recognition. *Proceedings of the IEEE*, 1998. 3
- [32] Junnan Li, Dongxu Li, Silvio Savarese, and Steven Hoi. Blip-2: Bootstrapping language-image pre-training with frozen image encoders and large language models. *arXiv preprint arXiv:2301.12597*, 2023. 1
- [33] Yanghao Li, Haoqi Fan, Ronghang Hu, Christoph Feichtenhofer, and Kaiming He. Scaling language-image pre-training via masking, 2022. 1, 3
- [34] Tsung-Yi Lin, Michael Maire, Serge Belongie, James Hays, Pietro Perona, Deva Ramanan, Piotr Dollár, and C Lawrence Zitnick. Microsoft coco: Common objects in context. In *European conference on computer vision*, pages 740–755. Springer, 2014. 4
- [35] Ilya Loshchilov and Frank Hutter. Decoupled weight decay regularization. In *ICLR*, 2019. 5, 6
- [36] Subhansu Maji, Esa Rahtu, Juho Kannala, Matthew Blaschko, and Andrea Vedaldi. Fine-grained visual classification of aircraft. *arXiv preprint arXiv:1306.5151*, 2013. 3
- [37] Maria-Elena Nilsback and Andrew Zisserman. Automated flower classification over a large number of classes. In *ICVGIP*, 2008. 3
- [38] Omkar M. Parkhi, Andrea Vedaldi, Andrew Zisserman, and C. V. Jawahar. Cats and dogs. In *CVPR*, 2012. 3
- [39] Alec Radford, Jong Wook Kim, Chris Hallacy, Aditya Ramesh, Gabriel Goh, Sandhini Agarwal, Girish Sastry, Amanda Askell, Pamela Mishkin, Jack Clark, et al. Learning transferable visual models from natural language supervision. In *ICML*, 2021. 1, 3
- [40] Samyam Rajbhandari, Jeff Rasley, Olatunji Ruwase, and Yuxiong He. Zero: Memory optimizations toward training trillion parameter models. In *SC20*, 2020. 2, 4, 5
- [41] Aditya Ramesh, Prafulla Dhariwal, Alex Nichol, Casey Chu, and Mark Chen. Hierarchical text-conditional image generation with clip latents. *arXiv preprint arXiv:2204.06125*, 2022. 1
- [42] Aditya Ramesh, Mikhail Pavlov, Gabriel Goh, Scott Gray, Chelsea Voss, Alec Radford, Mark Chen, and Ilya Sutskever. Zero-shot text-to-image generation. *arXiv preprint arXiv:2102.12092*, 2021. 5, 6
- [43] Jeff Rasley, Samyam Rajbhandari, Olatunji Ruwase, and Yuxiong He. Deepspeed: System optimizations enable training deep learning models with over 100 billion parameters. In *KDD*, 2020. 2, 4, 5, 6
- [44] Benjamin Recht, Rebecca Roelofs, Ludwig Schmidt, and Vaishaal Shankar. Do imagenet classifiers generalize to imagenet?, 2019. 3
- [45] Christoph Schuhmann, Romain Beaumont, Richard Vencu, Cade Gordon, Ross Wightman, Mehdi Cherti, Theo Coombes, Aarush Katta, Clayton Mullis, Mitchell Wortsman, et al. Laion-5b: An open large-scale dataset for training next generation image-text models. *arXiv preprint arXiv:2210.08402*, 2022. 1, 4, 6
- [46] Christoph Schuhmann, Richard Vencu, Romain Beaumont, Robert Kaczmarczyk, Clayton Mullis, Aarush Katta, Theo Coombes, Jenia Jitsev, and Aran Komatsuzaki. Laion-400m: Open dataset of clip-filtered 400 million image-text pairs. *arXiv preprint arXiv:2111.02114*, 2021. 5, 6
- [47] Khurram Soomro, Amir Roshan Zamir, and Mubarak Shah. Ucf101: A dataset of 101 human actions classes from videos in the wild. *arXiv preprint arXiv:1212.0402*, 2012. 4
- [48] Johannes Stallkamp, Marc Schlipsing, Jan Salmen, and Christian Igel. Man vs. computer: Benchmarking machine learning algorithms for traffic sign recognition. *Neural networks*, 2012. 3
- [49] Bastiaan S Veeling, Jasper Linmans, Jim Winkens, Taco Cohen, and Max Welling. Rotation equivariant cnns for digital pathology. In *MICCAI*, 2018. 3
- [50] Haohan Wang, Songwei Ge, Zachary Lipton, and Eric P Xing. Learning robust global representations by penalizing local predictive power. *NeurIPS*, 2019. 3
- [51] Jianxiong Xiao, James Hays, Krista A Ehinger, Aude Oliva, and Antonio Torralba. Sun database: Large-scale scene recognition from abbey to zoo. In *CVPR*, 2010. 3
- [52] Yang You, Jing Li, Sashank Reddi, Jonathan Hseu, Sanjiv Kumar, Srinadh Bhojanapalli, Xiaodan Song, James Demmel, Kurt Keutzer, and Cho-Jui Hsieh. Large batch optimization for deep learning: Training bert in 76 minutes, 2019. 1, 3, 5, 6
- [53] Peter Young, Alice Lai, Micah Hodosh, and Julia Hockenmaier. From image descriptions to visual denotations: New similarity metrics for semantic inference over event descriptions. *TACL*, 2014. 4